SELF-ASSEMBLED NANOCOMPOSITES

Jun Liu, Donghai Wang, Daiwon Choi, Gary Z. Yang, Vilayanur V. Viswanathan, Zimin Nie

Pacific Northwest National Laboratory, Richland, Washington, 99352

Introduction

Self-assembly is widely investigated to prepare nanoscale materials with desired architectures [1,2]. In particular, surfactant or polymer directed self-assembly has attracted great attention for ordered nanocomposites [1,2] and nanoporous materials [3,5]. Such self-assembled materials might have great potential for novel applications in electrical energy storage/conversion and electrocatalysis that require fast ion transport in the porous network [6]. For example, TiO_2 is an abundant, low cost, and environmentally benign material for anode applications in Li ion batteries. One drawback is that the poor lithium ionic and electronic conductivity of bulk TiO_2 polymorphs that limits their charge/discharge rate. To overcome the issue, TiO_2 polymorphs have been prepared as nanosized or nanoporous forms to reduce the Li-diffusion length in the solid phase and improve their cycling life due to minimized strain during lithium intercalation/deintercalation [7-9]. Nanoporous TiO_2 may also provide the additional advantages: 1) large surface area increases electrode/electrolyte contact area, which decreases the current density per unit surface area leading to higher charge/discharge rate; 2) nanopore structure provides short diffusion distance for both electron and Li^+ transport, permitting battery to use materials with low electronic/ionic conductivity [10-14]. The porous structure can also facilitate incorporation of secondary conducting components (e.g. carbon nanotube [15], SnO_2/CuO [16], RuO_2 [17]) within the nanoporous structure to enhance the electron conductivity of the materials and thus further improve high-rate charge-discharge performance. However, in general synthesis of stable, highly crystalline nanoporous materials and nanocomposites for energy using self-assembly methods remains a challenge.

Approaches

We will discuss our research on using self-assembly approaches to prepare stable nanoporous materials and nanocomposites for energy storage applications. For example, we developed a low-temperature solution growth of TiO_2 nanocrystals within an anionic surfactant matrix to produce highly crystalline mesoporous rutile and investigated Li intercalation properties of such nanoporous crystalline rutile [18]. To control the crystallization kinetics and the degree of cross-linking, we adapted a strategy for rutile synthesis in which the solubility and precipitation were controlled by hydrolysis and oxidation of titanium trichloride. Also, we found that the anions such as sulfate, whether present in the solution or derived from the precursor, have high affinity for chelating TiO_2. Based on these results, we chose anionic sulfate or sulfonic surfactants so that the strong binding with TiO_2 would keep the surfactant in the structure when the crystallization occurs. The processing parameters were optimized to obtain the highly crystalline nanoporous rutile nanostructures.

Results and Discussion

X-ray diffraction (XRD) patterns and N_2 sorption isotherms reveal nanoporous structure in the highly crystalline nanoporous TiO_2 directly results from the anionic surfactant templating effects with high surface area (245~300 m^2/g) and tunable mesopore diameter ranging from 2.2 to 3.8 nm after calcination. Transmission electron microscopy (TEM) measurements show that framework of the highly crystalline nanoporous TiO_2 are composed of aligned rutile nanorod building blocks grown along [001] direction (Figure 1a). The composite aggregates are all made of well-defined, “periodic” straight rod-like features. The rod-like features are oriented radially from central region towards the edges of the particle. High-resolution scanning electron microscopy (SEM) further confirms calcined sample is indeed composed of interspaced rod-like nanocrystals (Figure 1b). Detailed TEM studies further confirmed that the rod-like nanocrystals in MCTs are aligned or grown along [001] directions. As shown in Figure 1c, only parallel, (110) lattice fringes were observed along

the length of each rod-like nanocrystals identified by the spacing of adjacent lattice fringes equals to 0.32 nm, indicating that rutile nanocrystals were grown along [001] directions. Viewed in a different zone axis, Figure 1d shows the cross lattice fringe of (101) planes with good alignment over the entire region identified by 0.26 nm spacing of adjacent lattice fringes, which also confirm [001]-oriented rutile rod-like nanocrystals along its length. The new nanoporous crystalline rutile can accommodate more than 0.7 Li ($Li_{0.7}TiO_2$, 235 mAh/g) during the first charge at C/5 rate between 1–3 V versus Li^+/Li, with a reversible capacity of 0.55 Li ($Li_{0.55}TiO_2$, 185 mAh/g) (Figure 1e). The nanoporous crystalline rutile shows excellent capacity retention with less than 10% capacity loss after over 100 cycles (Figure 1f). XRD and TEM characterization on electrochemically lithiated sample show that the rutile nanorods were transformed into cubic rocksalt $LiTiO_2$ nanorods, but the mesoscale structures remained stable after the phase transformation and cycling.

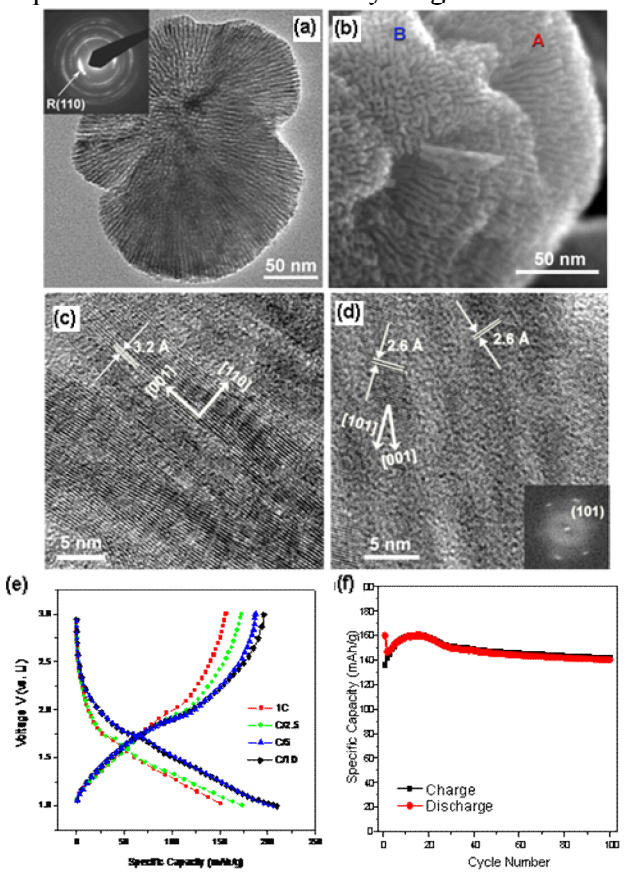

Figure 1. (a) TEM images of as-synthesized nanoporous rutile. (b) High-resolution SEM image of calcined sample. (c) and (d) High-resolution TEM image of calcined samples from different zone axis. (e) The 5th cycle discharge-charge capacity profile of the nanoporous crystalline TiO_2 at the various rate. (f) The cycling behavior of mesoporous crystalline TiO_2 up to 100 cycles at 1C rate.

We will also discuss our more recent work on incorporating conductive materials in the nanocomposites to further improve the functionality and performance of the energy storage materials. The ponetial of this approach to improve the mechanical and other properties will also addressed.

References

1. Decher, G. *Science* 277, 1232 (1997).
2. Whitesides, G. M., Mathias, J. P., C. T. Seto, C. T. *Science* 254, 1312 (1991).
3. Kresge, C. T., Leonowicz, M. E., Roth, W. J., Vartuli, J. C., Beck, J. S. *Nature* 359, 710 (1992).
4. Bagshaw, S. A., Prouzet, E., Pinnavaia, T. J. *Science* 269, 1242 (1995).
5. Zhao, D. Y., Feng, J. L., Huo, Q. S. Melosh, N., Fredrickson, Chmelka, B. F., Stucky, G. D., *Science* 279, 548 (1998).
6. Liu, J., Cao, G., Yang, G., Wang, D. H., Dubois, D., Zhou, X., Graff, G. L., Pederson, L. R., Zhang, J. G. *ChemSusChem*, online (2008).
7. Maier, J., *Nature Materials* 2005, *4*, 805.
8. Wang, Y.; Cao, G. Z., *Chemistry of Materials* 2006, *18*, 2787.
9. Sides, C. R.; Li, N. C.; Patrissi, C. J.; Scrosati, B.; Martin, C. R., *Mrs Bulletin* 2002, *27*, 604.
10. Attia, A.; Zukalova, M.; Rathousky, J.; Zukal, A.; Kavan, L., *Journal of Solid State Electrochemistry* 2005, *9*, 138.
11. Moriguchi, I.; Hidaka, R.; Yamada, H.; Kudo, T., *Solid State Ionics* 2005, *176*, 2361.
12. Guo, Y. G.; Hu, Y. S.; Maier, J., *Chemical Communications* 2006, 2783.
13. Kavan, L.; Rathousky, J.; Gratzel, M.; Shklover, V.; Zukal, A., *Journal of Physical Chemistry B* 2000, *104*, 12012.
14. Kavan, L.; Attia, A.; Lenzmann, F.; Elder, S. H.; Gratzel, M., *Journal of the Electrochemical Society* 2000, *147*, 2897.
15. Moriguchi, I.; Hidaka, R.; Yamada, H.; Kudo, T.; Murakami, H.; Nakashima, N., *Advanced Materials* 2006, *18*, 69.
16. Zhou, H. S.; Li, D. L.; Hibino, M.; Honma, I., *Angewandte Chemie-International Edition* 2005, *44*, 797.
17. Guo, Y. G.; Hu, Y. S.; Sigle, W.; Maier, J., *Advanced Materials* 2007, *19*, 2087.
18. Wang, D. H. Choi, D. W. Yang, Z. G. Viswanathan, V. V, Nie, Z. M., Wang, C. M. Song, Y. J., Zhang, J. G., Liu, J. *Chem. Mat.*, 20, 3435-3442, 2008.